



## OPEN ACCESS

## EDITED BY

Sandeep Kumar,  
Nagoya University, Japan

## REVIEWED BY

Yuichi Otsuka,  
Nagoya University, Japan  
Bharati Kakad,  
Indian Institute of Geomagnetism (IIG), India

## \*CORRESPONDENCE

Bela G. Fejer,  
✉ [bela.fejer@usu.edu](mailto:bela.fejer@usu.edu)

RECEIVED 06 December 2023

ACCEPTED 24 January 2024

PUBLISHED 06 February 2024

## CITATION

Fejer BG, Laranja SR and Condor P (2024),  
Multi-process driven unusually large  
equatorial perturbation electric fields during  
the April 2023 geomagnetic storm.  
*Front. Astron. Space Sci.* 11:1351735.  
doi: 10.3389/fspas.2024.1351735

## COPYRIGHT

© 2024 Fejer, Laranja and Condor. This is an  
open-access article distributed under the  
terms of the [Creative Commons Attribution  
License \(CC BY\)](https://creativecommons.org/licenses/by/4.0/). The use, distribution or  
reproduction in other forums is permitted,  
provided the original author(s) and the  
copyright owner(s) are credited and that the  
original publication in this journal is cited, in  
accordance with accepted academic practice.  
No use, distribution or reproduction is  
permitted which does not comply with  
these terms.

# Multi-process driven unusually large equatorial perturbation electric fields during the April 2023 geomagnetic storm

Bela G. Fejer<sup>1\*</sup>, Sophia R. Laranja<sup>2,3</sup> and Percy Condor<sup>4</sup>

<sup>1</sup>Center for Atmospheric and Space Sciences, Utah State University, Logan, UT, United States,

<sup>2</sup>Department of Electrical and Computer Engineering, Utah State University, Logan, UT, United States,

<sup>3</sup>Space Sciences Laboratory, Aeronautics Institute of Technology, São José dos Campos, Brazil,

<sup>4</sup>Jicamarca Radio Observatory, Instituto Geofísico del Perú, Lima, Peru

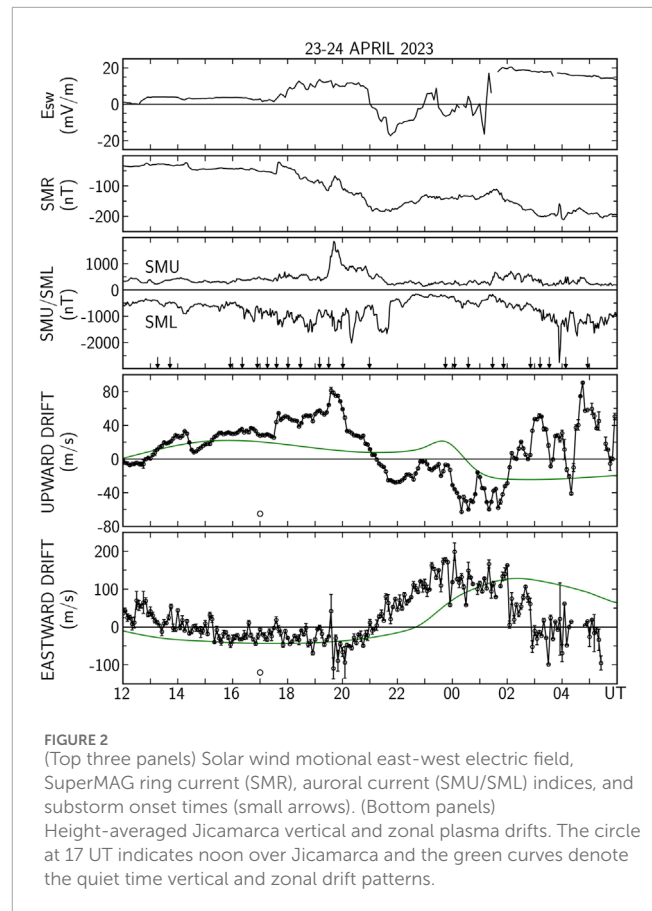
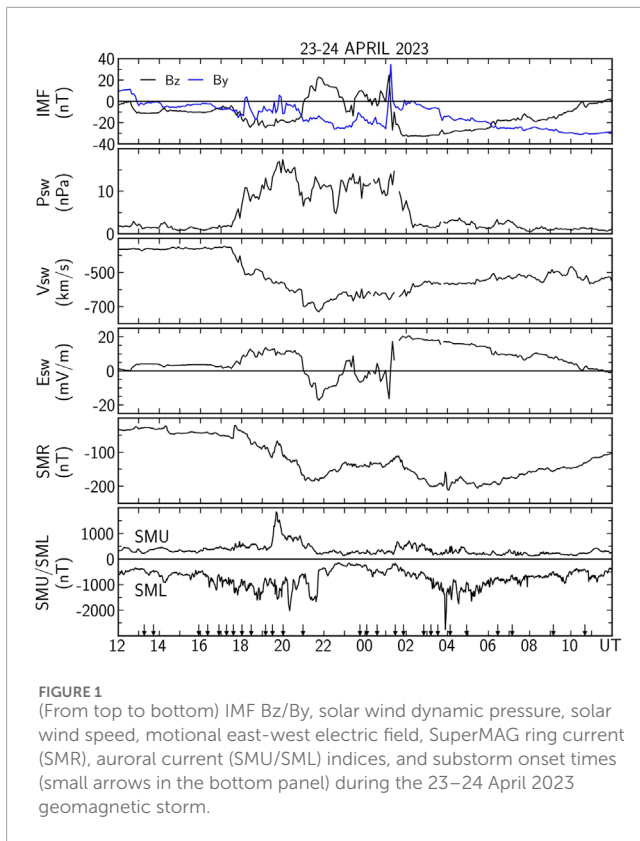
The low latitude ionosphere and thermosphere are strongly disturbed during and shortly after geomagnetic storms. We use novel Jicamarca radar measurements, ACE satellite solar wind, and SuperMAG geomagnetic field observations to study the electrodynamic response of the equatorial ionosphere to the 23, 24 April 2023 geomagnetic storm. We also compare our data with results from previous experimental and modeling studies of equatorial storm-time electrodynamic. We show, for the first time, unusually large equatorial vertical and zonal plasma drift (zonal and meridional electric field) perturbations driven simultaneously by multi storm-time electric field mechanisms during both the storm main and recovery phases. These include daytime undershielding and overshielding prompt penetration electric fields driven by solar wind electric fields and dynamic pressure changes, substorms, as well as disturbance dynamo electric fields, which are not well reproduced by current empirical models. Our nighttime measurements, over an extended period of large and slowly decreasing southward IMF Bz, show very large, substorm-driven, vertical and zonal drift fluctuations superposed on large undershield driven upward and westward drifts up to about 01 LT, and the occurrence of equatorial spread F irregularities with very strong spatial and temporal structuring. These nighttime observations cannot be explained by present models of equatorial storm-time electrodynamic.

## KEYWORDS

equatorial ionosphere, ionospheric disturbances, ionosphere/magnetosphere interactions, electric fields, ionospheric irregularities

## 1 Introduction

Interplanetary magnetic field (IMF) driven ionospheric electrodynamic disturbances extending from high to equatorial latitudes have been studied for several decades (e.g., Matsushita, 1953; Rastogi, 1962; Nishida, 1968). Starting in the early 1970s, newly developed ionospheric radar measurements led to significantly more detailed studies of the response of middle and low latitude ionospheric electric fields to geomagnetic disturbances (e.g., Matsushita and Balsley, 1973; Chandra and Rastogi, 1974; Rastogi and Patel, 1975; Fejer et al., 1976; Blanc, 1978). They also showed that IMF driven large-scale magnetospheric electric fields imposed on the high-latitude ionosphere can be transmitted



nearly instantaneously to middle and low latitudes through the Earth-ionosphere waveguide (e.g., Kikuchi et al., 1978).

In a landmark study, Kelley et al. (1979) pointed out that anomalous equatorial zonal ionospheric electric field reversals were associated with sudden changes in the magnetospheric convection electric field driven by rapid IMF northward turnings from steady southward direction. Extensive follow up radar, magnetometer, and ionosonde studies examined in detail the effects of IMF and high-latitude current systems on nearly simultaneous middle and low latitude ionospheric electric field and current perturbations (e.g., Fejer et al., 1979; Gonzales et al., 1979; Gonzales et al., 1983; Reddy et al., 1979; Fejer, 1997; Kikuchi et al., 2003). These short-lived storm-time disturbance electric fields, commonly referred to as prompt penetration electric fields, have lifetimes from a few minutes to a few hours. They are driven mostly by rapid IMF Bz fluctuations which cause a temporary imbalance between region 1 and region 2 Birkeland currents resulting in sudden changes in magnetospheric convection and in meridional motions of the nighttime shielding layer (e.g., Wolf et al., 1982; Spiro and Wolf, 1984; Spiro et al., 1988). Convection increases (decreases) drive upward and westward (downward and eastward) drifts during the day and with opposite polarity at night with highest amplitudes shortly before their sign reversals near sunrise and sunset (e.g., Fejer and Scherliess, 1997; Fejer, 2011).

Low latitude prompt penetration electric fields are also driven by magnetospheric substorms, solar wind dynamic pressure changes, solar flares, and Ultra Low Frequency (ULF) waves (Chakrabarty et al., 2008; Chakrabarty et al., 2015; Wei et al., 2015; Veenadhari et al., 2019; Huang, 2020; Fejer et al., 2021;

Fejer and Navarro, 2022). During periods of southward IMF Bz, magnetospheric substorm onset and expansion phases are associated with eastward daytime and westward nighttime prompt penetration electric fields (e.g., Huang, 2012; Huang, 2020; Tulasi Ram et al., 2016; Fejer and Navarro, 2022). Slower varying and longer lasting (lifetimes from a few hours to a few days) middle and low latitude disturbance electric fields during and shortly after strong geomagnetic disturbances result from thermospheric disturbance wind dynamo effects (e.g., Blanc and Richmond, 1980; Fejer et al., 1983; Fejer et al., 2017; Fejer, 1991; Navarro et al., 2019). During magnetic storms, ionospheric disturbance electric fields result from complex interactions of multi-source driven prompt penetration and disturbance dynamo electric fields (e.g., Maruyama et al., 2005; Fejer et al., 2007).

Prompt penetration and disturbance electric fields have long been known to significantly affect the generation and evolution of equatorial nighttime F-region plasma irregularities by changing the instability growth rate (e.g., Rastogi et al., 1978; Fejer et al., 1999; Abdu, 2012). Substorms were recently shown to cause strong structuring on equatorial spread F (e.g., Fejer et al., 2021; Sori et al., 2022; Sousasantos et al., 2023). Storm-time ionospheric electric field also have major effects on the temporal and spatial variation of ionospheric plasma from auroral to equatorial latitudes (e.g., Astafyeva et al., 2016; Aa et al., 2018). In the nighttime sector, strong prompt penetration driven equatorial plasma depletions can rise to apex heights over 6,000 km and merge with midlatitude Traveling Ionospheric Disturbances (TIDs) (e.g., Aa et al., 2019).

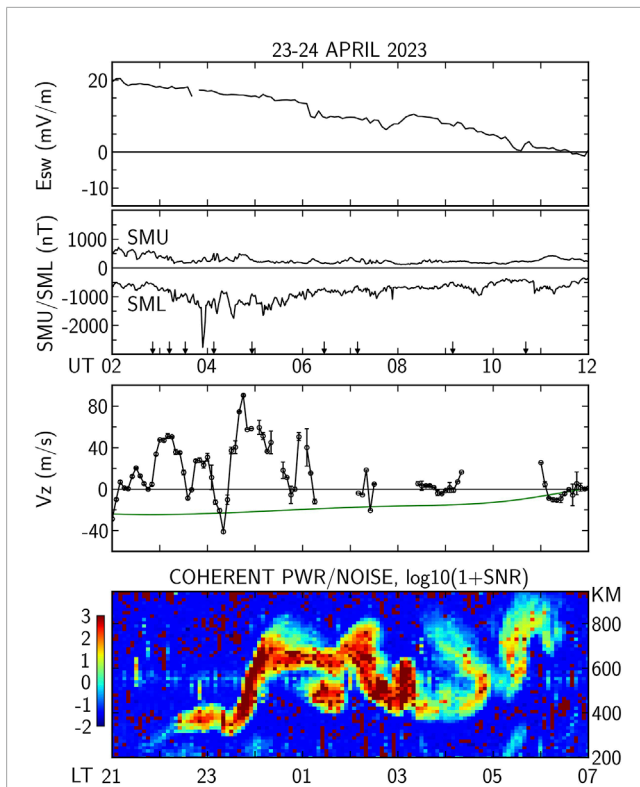


**FIGURE 3** (Top two panels) Solar wind motional east-west electric field, auroral current (SMU/SML) indices, and substorm onset times (small arrows). (Third panel) Height-averaged Jicamarca vertical plasma drifts and their quiet-time values (green curve). (Fourth panel) Coherent backscattered power from 3-m plasma density irregularities.

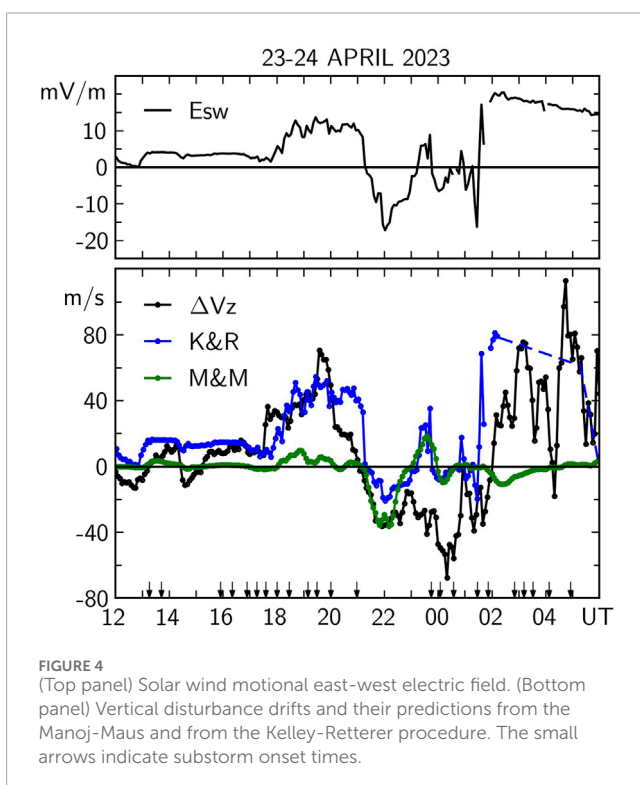


**FIGURE 4** (Top panel) Solar wind motional east-west electric field. (Bottom panel) Vertical disturbance drifts and their predictions from the Manoj-Maus and from the Kelley-Retterer procedure. The small arrows indicate substorm onset times.

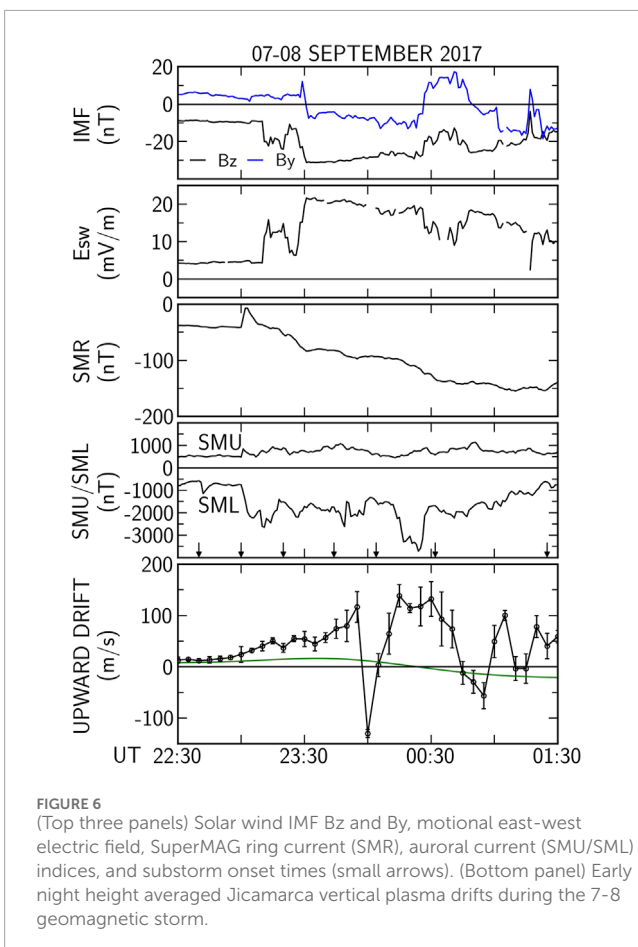
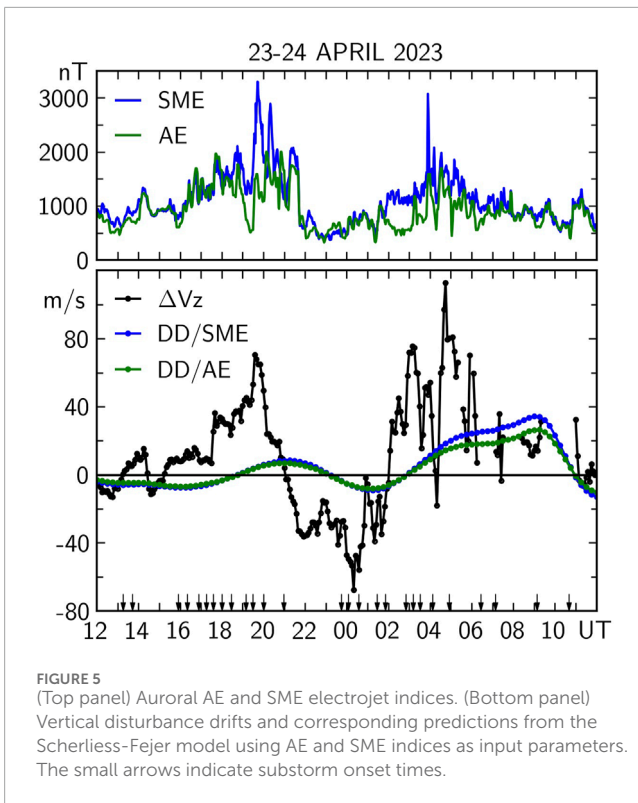
In this paper, we used radar measurements from the Jicamarca Radio Observatory (11.9°S, 76.8°W; dip latitude ~0°), solar wind parameters, and ground-based magnetometer data to study the unusual electrodynamic response of the equatorial ionosphere to the 23–24 April 2023 large geomagnetic storm. In the following sections, we first describe our novel radar operating mode and data analysis, and then proceed to describe and discuss our results.

## 2 Measurement techniques and data

We used novel Jicamarca incoherent scatter medium power (ISR MP) radar measurements of F-region  $E \times B$  plasma drifts and spread-F irregularities, ACE satellite solar wind, and SuperMAG ground-based magnetic field measurements from 12 UT (07 LT) 23 April 2023 to 12 UT 24 April 2023. The ISR MP mode is one of the novel Jicamarca Unattended Long-term Investigations of the Ionosphere and Atmosphere Medium Power (JULIA MP) modes which consists in using 2 new solid-state transmitters of 96 kW peak power each instead of the 4 large 1.5 MW transmitters used for over seven decades at Jicamarca (Kuyeng et al., 2023). This lower power (and lower operational cost) mode, operated with a 10% duty cycle, allows for nearly continuous operation of the radar. The obvious handicap is that, under low plasma density conditions (e.g., after about midnight), the incoherent scatter measurements have very large errors. In the ISR MP mode, the interpulse period (IPP) is 1,500 km, the pulse length is 45 km, and the radar beams are directed about 2.4° eastward and 4.3° westward in the plane perpendicular to the magnetic field. The data acquisition and signal processing techniques and the procedure for deriving the vertical (positive upward) and zonal plasma (positive eastward) drifts from the line-of-sight values are the same as in standard Jicamarca radar drift experiments. These were described by Kudeki et al. (1999) and Woodman (1970), respectively.

The Jicamarca drift experiments also provide temporal and spatial information on nighttime small-scale (3-m) equatorial spread F plasma irregularities. However, ambient F-region plasma drifts cannot be reliably derived in regions of strong spread F echoes and when the plasma is strongly inhomogeneous in the east-west plane over the altitudinal range of about ~200–800 km. Therefore, measurements from these coherent scatter regions are routinely removed from the Jicamarca drift. In the present study, we used 5-min spread-F free drifts averaged from 250 to 500 km for the vertical component and from 250 to 450 km for the zonal. We deleted height averaged drifts with standard deviations larger than 30 and 100 m/s for the vertical and zonal components, respectively, and zonal drifts with magnitudes larger than 200 m/s. The standard deviations of our height averaged drifts are ~1 during the day and ~10 m/s during the night (up to ~06 UT) for the vertical component, and ~10 m/s during the day and ~25 m/s at night (up to ~04 UT) for the zonal. Over Jicamarca, an eastward (northward) electric field of 1 mV/m corresponds to an upward (westward) drift of ~40 m/s.

We also used 5-min Advanced Composition Explorer (ACE) satellite solar wind measurements of the GSM Y and Z components of the interplanetary magnetic field (IMF), solar wind dynamic pressure and speed, and Y (east-west) component of the motional solar wind electric field time-propagated to the noon magnetopause obtained from the NASA Goddard database (<https://omniweb>).



gsfc.nasa.gov/), and also ground-based ring current and auroral magnetic field SMR, SMU, SML, and SME (equivalent to the SYM-H/Dst, AU, AL, and AE) indices obtained from the SuperMAG database (<http://supermag.jhuapl.edu/>). These geomagnetic indices were derived from ~300 ground-based magnetometer data with a temporal resolution of 1 min (Gjerloev, 2012). The preliminary AE indices were obtained from the World Data Center (WDC) for Geomagnetism, Kyoto AE index service.

### 3 Results

Figure 1 shows solar wind parameters from the ACE satellite and geomagnetic indices from SuperMAG measured during the 23–24 April 2023 severe geomagnetic storm. This coronal mass ejection (CME) driven storm started at 09 UT on the 23rd. Following the initial slow strengthening of the southward IMF Bz and increase of the ring current, the storm became strong after 1737 UT. The storm first main phase lasted up to ~2140 UT with the SMR ring current index reaching a minimum of –184 nT. In the second main phase, which lasted from 0134 to 0407 UT on the 24th, the SMR had a minimum of –203 nT at 0403 UT. The Kp index reached values of 8+ and 8 during the first and second storm main phases, respectively.

Figure 1 shows that the IMF Bz was southward and nearly steady with values of ~10 nT up to about 1737 UT when it turned increasingly southward reaching about –20 nT at 1820 UT. Later, it did not change much up to ~21 UT when it first turned strongly northward, and then decreased to small northward and southward values for ~3 h. After large northward and southward variations at ~01 UT, the IMF Bz became strongly southward to about –30 nT, and then slowly decreased up to ~12 UT on the 24th. The IMF By had generally small values up to ~20 UT, was ~–20 nT up to ~01 UT when it underwent sign changes before becoming very small, and then turning steadily negative (toward dusk) up to ~11 UT on the 24th. The solar wind dynamic pressure had large values and amplitude fluctuations from ~28 UT on the 23rd to ~02 UT on the 24th. The solar wind speed increased strongly from ~1730 UT to 22 UT on the 23rd, which is indicative of strong solar wind-magnetosphere coupling conditions (e.g., Newell et al., 2008), and then decreased slowly. The solar wind motional electric field was weakly eastward prior to ~1,730 UT when it increased to ~10 mV/m up to ~21 UT on the 23rd, then it turned strongly westward up to ~23 UT on the 23rd before oscillating with small amplitudes up to ~01 UT on the 24th. Later, it underwent large amplitude fluctuations followed by a large eastward increase and a slow gradual decrease up to ~11 UT on the 24th. The SMU was ~500 nT on the 23rd, underwent a large increase associated with the large corresponding increase in the dynamic pressure during 19–20 UT on the 23rd, and had generally small values afterwards. The SML values were large and with large fluctuations indicating significant substorm activity with their onset times indicated by small arrows. Figure 1 shows numerous fast recurring (quasi-periods of ~30 min) substorms from ~16 UT to the end of the storm first main phase (~22 UT) and from ~2340 UT to ~05 UT on the 24th. Later, there were also a few more substorms up to ~11 UT on the 24th.

Figure 2 presents again in the three top panels the ACE solar wind electric field and the SuperMAG ring current and auroral

geomagnetic indices with substorm onset times. The fourth and fifth panels show the height averaged Jicamarca vertical and zonal plasma drifts with their standard deviations superposed on the corresponding quiet-time drift patterns. Figure 2 indicates that, prior to the storm onset, there were generally only small equatorial upward and eastward perturbation drifts over Jicamarca. The sudden increase of geomagnetic activity at 1737 UT resulted in an initial rapid increase followed by a nearly steady decrease of the ring current index over the storm first main phase. In this period, the upward perturbation drifts increased first rapidly, at the storm onset, and then more slowly up to ~1930 UT when they increased strongly again, likely due to the large increase in the solar wind dynamic pressure (see Figure 1) and resulting increase in the SMU index. The corresponding short-lived vertical perturbation drifts, which are indicative of undershielding prompt penetration and substorm activity, lasted up to ~21 UT when the solar wind electric field reversed following the IMF Bz strong northward turning. Over this main storm phase, the equatorial zonal drifts did not show significant disturbance effects, except for the large and very brief first eastward and then westward perturbations at ~1930 UT, when the vertical drifts changed rapidly in response to the large sudden change in the solar wind dynamic pressure.

The solar wind electric field was mostly westward from ~21 UT on the 23rd to ~01 UT on the 24th, except for brief and fast eastward turnings. Over this period, the equatorial vertical perturbation drifts were strongly downward, in general, due to westward disturbance dynamo and prompt penetration electric fields with occasional upward perturbation fields (e.g., near 2300 UT and 0030 UT). Figure 2 shows very large eastward disturbance drifts over this period, and also brief large eastward and westward drift perturbations during times of rapid vertical drift changes. The large and slowly varying late afternoon to early evening eastward disturbance dynamo drifts in Figure 2 are the largest ever recorded at Jicamarca over this period.

Figure 1 shows very large fluctuations in IMF Bz and By at ~01 UT, near the onset of the storm brief second main phase. Later, the initially very large southward IMF Bz slowly decreased up to 11 UT on the 24th, and the initially very small westward IMF By systematically increased to about ~30 nT. From 0130 to 06 UT, the corresponding solar wind eastward electric field changed from 20 to 16 mV/m. Over this period, Figure 2 shows very large, substorm driven, vertical and zonal drift fluctuations superposed on large undershielding driven upward and westward drifts up to about 01 LT. Substorm driven perturbations were particularly strong during ~03–05 UT with vertical drift fluctuations of ~120 m/s at ~0430 UT. We will point out later that disturbance dynamo electric fields did not appear to have contributed significantly to the nighttime upward drifts before ~04 UT. This pre-midnight period highlights simultaneous very large contributions from multiple storm-time electro-dynamical mechanisms to equatorial disturbance electric fields. As noted earlier, the errors on the drift measurements were significantly larger in the post-midnight sector due to very low signal-to-noise ratios.

Figure 3 shows from top to bottom the solar wind electric field, auroral electrojet indices, Jicamarca vertical drifts, and backscattered power from 3-m equatorial spread F plasma irregularities from 02 to 09 UT. We note that measurements from these coherent scatter

regions were not used in estimating the plasma drifts. Spread F irregularities first developed at ~0330 UT (2230 LT) following the vertical drift reversal to upward, they weakened at 0420 UT with the reversal to downward, and then strengthened strongly and rapidly rose to ~700 km following the large increase of the upward drifts at ~0440 UT. Later, their height range and strength varied considerably up to 0820 UT most likely due to highly variable vertical drifts likely caused by strong substorm activity. The weak late night and early morning irregularities were likely driven by disturbance dynamo drifts, as discussed below.

## 4 Discussion

The interplanetary motional electric field and disturbance dynamo electric field have long been known to play major roles on equatorial storm-time plasma drifts (e.g., Kelley et al., 1979; Blanc and Richmond, 1980; Fejer and Scherliess, 1997). In this section, we initially examine to what extent our disturbance drifts, obtained by removing the corresponding quiet-time values, can be explained by prompt penetration disturbance dynamo drifts predicted by empirical electric field models. Then, we briefly discuss processes possibly responsible for our early night unusual plasma drift observations.

Three empirical vertical drift models have been widely used in storm-time equatorial electric field studies. The Fejer and Scherliess (1997) model estimates equatorial storm-time prompt penetration and disturbance dynamo vertical drifts using times series of 15 min averaged AE indices over the previous 28 h and transfer functions derived from extensive Jicamarca radar measurements. The other two widely used equatorial storm-time empirical models both use ACE measured solar wind electric fields to infer equatorial prompt penetration electric fields (vertical plasma drifts). They were motivated by numerous earlier studies pointing out that the magnetosphere-ionosphere system generally acts like a high-pass filter in response to solar wind electric field variability (e.g., Kelley, 1989; Huang et al., 2007; Nicolls et al., 2007). Based on a number of earlier studies, Kelley and Retterer (2008) suggested that, on average, the ratio of the equatorial zonal prompt penetration electric field to the dawn-to-dusk interplanetary electric field is 0.1 for southward IMF and 0.03 for northward IMF. This parametrization, referred here as the Kelley-Retterer (K-R) model, have been used in a number of follow up studies of daytime equatorial prompt penetration electric fields (e.g., Huang, 2019; Huang, 2020; Huang and Zhang, 2021). The other solar wind electric field based equatorial zonal prompt penetration electric field model was developed by Manoj et al. (2008). Manoj and Maus (2012) combined the outputs of the Manoj et al. (2008) and Scherliess and Fejer (1999) quiet-time vertical drift model to provide real time global equatorial zonal electric field predictions. The predictions from this model are available at <http://www.geomag.us/models/PPEFM>.

Figure 4 shows, in the top panel, the solar wind electric field for the period illustrated in Figure 2. The bottom panel shows daytime and evening vertical drift perturbations obtained from Figure 2 by removing the corresponding quiet-time values, the prompt penetration drifts derived using the prescription suggested by Kelley and Retterer (2008) and shifted by 17 min to account the propagation time from the front of the magnetopause to

the equatorial ionosphere, and the corresponding results from the [Manoj and Maus \(2012\)](#) model. Although the K-R model does not specify when the early night undershielding electric fields change from upward to downward, in [Figure 4](#) we extended its daytime prescription up to 06 UT (01 LT) considering our very large corresponding measured upward drifts. We note that, in addition to prompt penetration electric fields, the residual drifts were also clearly affected by other processes including dynamic pressure changes, substorms and disturbance dynamo electric fields.

For this storm, Fejer-Scherliess model predicts prompt penetration vertical drifts (not shown) with the correct sign, but with much smaller amplitudes than inferred from [Figure 4](#). This confirms earlier results indicating that this model is generally not well suited for accurate modeling this highly dynamic storm-time parameter. The longer-lived disturbance dynamo zonal electric field predicted by this model for the 23–24 April storm will be discussed later. [Figure 4](#) indicates that the equatorial daytime short-lived perturbation drifts are generally in reasonable agreement with the prediction of the K-R model. We note that this is often not the case. On the other hand, the [Manoj and Maus \(2012\)](#) model disturbance drifts, which are proportional to the average time rate of change of the solar wind electric field, significantly underestimate the observed prompt penetration electric fields except between before about ~21–24 UT (16–19 LT).

The solar wind dynamic pressure was very strong and highly variable during ~18–02 UT (13–21 LT), as indicated in [Figure 1](#). Over this period, [Figures 2, 4](#) show noticeable short-lived penetration electric fields associated with dynamic pressure changes and related substorm activity. Solar wind dynamic pressure increases drive equatorial upward and westward plasma drifts (eastward and northward electric fields) during the day (e.g., [Tsunomura, 1999](#); [Fejer and Emmert, 2003](#); [Huang, 2020](#)). The very large increase in SMU and upward drifts at ~1940 UT, in particular, was associated with a fast and large increase in the solar wind dynamic pressure. In this case, the corresponding westward drift perturbation is not as clear probably due to larger measurement errors. Numerous substorms also occurred between 13 and 21 LT, as indicated in [Figure 4](#). Magnetospheric substorms generally drive only small daytime equatorial upward drifts. The strong substorm during ~2,120–2135 UT, for example, just appear to have slowed down the decrease of the upward drift following the sudden weakening of the southward IMF Bz and solar wind electric field.

[Figure 5](#) shows in the top panel the preliminary WDC-Kyoto AE and the SME indices for the 23–24 geomagnetic storm. The bottom panel presents the daytime and early night Jicamarca perturbation drifts, and the corresponding disturbance dynamo vertical drifts predicted by the [Scherliess and Fejer \(1997\)](#) model. Surprisingly, during this large storm, both auroral indices are generally in good agreement. [Figure 5](#) shows that the Scherliess-Fejer model predicts only very small disturbance dynamo drifts up to ~04 UT (~23 LT) and increasing upward drifts thereafter up to ~09 UT (04 LT). The model does not predict, in particular, the large disturbance downward drifts between ~21–02 UT (~16–21 LT), which cannot be fully accounted for by overshielding prompt penetration electric field effects. As mentioned earlier, over these periods, the large eastward drift perturbations shown in [Figure 2](#) are

indicative of strong disturbance dynamo effects. We also note that strong downward evening drift perturbations are a climatological feature of the equatorial disturbance dynamo mechanism (e.g., [Fejer, 2002](#); [Navarro et al., 2019](#)). Overall, these results clearly confirm that the equatorial disturbance dynamo electric fields during this storm were also highly unusual.

[Figures 2, 5](#) showed unusually large and highly variable perturbation plasma drifts during ~02–06 UT (~21–01 LT). [Fejer et al. \(2021\)](#) used Jicamarca radar measurements during the 8 September 2017 large geomagnetic storm to highlight, for the first time, very large early night equatorial vertical drift fluctuations during a period of strong southward IMF Bz. They suggested that these prompt penetration drifts were caused by strong substorm activity and rapid dipolarization of magnetotail field lines during IMF By recovery (e.g., [Kokubun and McPherron, 1981](#); [Wolf et al., 1982](#); [Fejer et al., 1990](#)). This September 2017 event is illustrated again in [Figure 6](#) now using reanalyzed measurements. In contrast to the September 2017 nighttime substorm event, however, the very large vertical drift perturbations in the early night of 23 April 2023 were associated with steadily increasing westward IMF By instead of its recovery. We note that the amplitudes of the nighttime prompt penetration vertical drifts associated with the 7–8 September 2017 and 23–24 April 2023 substorms were much larger than those associated with daytime magnetospheric substorms measured under similar geophysical conditions, under such large southward IMF Bz. The amplitudes of the daytime substorm-driven vertical prompt penetration drifts during the main phase of the 8 September 2017 large magnetic storm, for example, were generally smaller than 20 m/s ([Fejer and Navarro, 2022](#)). This suggests that magnetospheric storm-time substorms drive larger equatorial prompt penetration electric field in the premidnight sector than during daytime.

[Fejer et al. \(2021\)](#) pointed out that the September 2017 substorm event was also associated with strong temporal and spatial structuring of equatorial spread F irregularities. [Figures 2, 3](#) strongly suggest that this was also the case for the spread F irregularities observed during the 23–24 April 2023 geomagnetic storm. This strong plasma irregularity structuring should cause strong spatial and temporal variability on low latitude TEC latitudinal profiles. We note that the drift velocities of the measured 3-m plasma irregularities cannot be determined with our radar operating mode.

Numerous model and experimental studies indicated that during southward IMF Bz the evening and early night equatorial prompt penetration vertical plasma drifts (zonal electric fields) are upward (eastward) up to about 22 LT with peak upward drifts (eastward electric fields) at ~19 LT (e.g., [Tsunomura and Araki, 1984](#); [Senior and Blanc, 1987](#); [Spiro et al., 1988](#); [Fejer et al., 1990](#); [Fejer et al., 2008](#); [Fejer and Scherliess, 1997](#); [Tsunomura, 1999](#); [Sazykin, 2000](#); [Huang, 2015](#); [Huang, 2020](#)). As pointed out earlier, disturbance dynamo effects are unlikely to have affected the 23–24 April 2023 storm late night vertical drift reversal. Therefore, the occurrence of mostly upward vertical drifts up to ~01 LT during strong southward IMF Bz and undershielding conditions on the 23 April 2023 storm is highly unusual. To the best of our knowledge, the only similar event reported occurred during the 7–10 November 2004 very large magnetic storm when on the 10th, under strongly southward IMF Bz, the Jicamarca vertical drifts

reversed to downward at ~01–02 LT (06–07 UT) (e.g., Fejer et al., 2007; Kelley and Retterer, 2008; Kelley et al., 2010; Lu et al., 2012; Huang and Zhang, 2021). As in our case, the IMF By was also strongly negative during the 10 November 2004 storm late vertical drift reversal. Unpublished Jicamarca radar measurements during the 13–14 December large geomagnetic storm indicate that under steady southward IMF Bz and frequent substorm activity, the vertical drift reversal to downward occurred near local midnight. In this latter case, however, the IMF By was very small. These three storm-time late equatorial undershielding driven vertical drift reversal events suggest highly unusual solar wind-magnetospheric-ionospheric conditions.

Wolf (1970) pointed out that mid- and low-latitude magnetospheric dynamo electric fields are controlled by the high-latitude convection and potential distribution, driven by magnetic field aligned (Birkeland) currents, and strongly affected by longitudinal and latitudinal variation of high latitude Pedersen and Hall conductances. The divergence-free condition for the ionospheric currents leads to poleward (equatorward) gradients in the meridional electric field near dusk (dawn). Furthermore, the enhanced auroral conductivities cause an eastward rotation of the high latitude potential distribution (Wolf, 1970; Riley, 1994). The combined effect of these processes is illustrated in Figure 6 of Fejer (1997). Phase changes of the polar cap potential distribution have significant effects on mid- and low-latitude magnetospheric electric fields near to dawn and dusk (Wolf et al., 1982; Blanc, 1983; Senior and Blanc, 1987). RCM simulations presented by Sazykin (2000) indicate that a rotation of the high latitude potential distribution to later local times increases the premidnight eastward and southward prompt penetration electric fields at all latitudes. These simulations indicate that a 2-h rotation of the potential to later local times cause the eastward to westward nighttime electric field reversal to occur close to 24 MLT. In this case, the simulation also indicates increased southward electric field (i.e., westward drifts) in the premidnight sector, which is consistent with the results in Figure 2.

Rotations of the high latitude convection in local time have been associated to solar cycle and seasonal changes and with IMF By sign and magnitude changes. However, since these rotations have opposite signs in the northern and southern high latitudes it is not clear how they could explain our observations. We speculate that strongly substorm activity and unusual high-latitude conductances in the early night period have a significant role on late night undershielding-driven vertical drift reversals. Clearly, additional experimental and modeling studies are needed to explain our complex observations.

In summary, we showed that very large equatorial disturbance vertical and zonal plasma drifts were observed during the 23–24 large geomagnetic storm. The daytime disturbance prompt penetration vertical drifts were generally proportional to changes in the solar wind electric field but were also strongly affected by solar wind dynamic pressure changes, and possibly by substorms and disturbance dynamo electric fields. As is often the case, the relative contributions of these different disturbance processes cannot be fully determined. In terms of storm-time electrodynamic studies, however, the main limitation of local time empirical equatorial electrodynamic models (e.g., K-R and Manoj-Maus) is that they do not fully take into account the near past history

of geomagnetic activity which can significantly precondition the ionospheric response.

The nighttime measurements showed unusually large amplitude substorm-driven prompt penetration vertical drifts superposed on large undershielding upward drifts up to about midnight, which are not well reproduced by either current empirical or theoretical models. Our results also suggest that the substorm-driven prompt penetration electric field efficiency is much higher in the premidnight sector than during the day. These short-lived substorms significantly modulate the growth rate of the Rayleigh-Taylor instability and therefore the structuring of equatorial and low latitude spread-F irregularities. The development of magnetospheric convection models including magnetospheric substorms and extending down to equatorial latitudes is clearly needed for improved predictions of the global ionospheric response to magnetic storms.

## Data availability statement

The datasets presented in this study can be found in online repositories. The names of the repository/repositories and accession number(s) can be found below: <https://doi.org/10.5281/zenodo.10257723>.

## Author contributions

BF: Conceptualization, Formal Analysis, Funding acquisition, Investigation, Methodology, Validation, Visualization, Writing—original draft, Writing—review and editing. SL: Formal Analysis, Software, Validation, Writing—original draft, Writing—review and editing. PC: Data curation, Writing—review and editing.

## Funding

The author(s) declare financial support was received for the research, authorship, and/or publication of this article. The research at Utah State University was funded by NASA grants 80MSFC18C0010 and 80NSSC17K071. SL was supported by the Coordenação de Aperfeiçoamento de Pessoal de Nível Superior - Brazil (CAPES)—Financing Code 001 under the process 88881.676788/2022-01.

## Acknowledgments

We thank the Jicamarca staff and K. Kuyeng in particular. We also thank L. Navarro and J. Evans for the helpful comments. The Jicamarca Radio Observatory is a facility of the Instituto Geofísico del Perú operated with support from NSF award AGS-1732209 through Cornell University. We acknowledge the substorm timing list identified by the Newell and Gjerloev technique (Newell and Gjerloev, 2011), the SMU and SML indices

(Newell and Gjerloev, 2011); and the SuperMAG collaboration (Gjerloev, 2012).

## Conflict of interest

The authors declare that the research was conducted in the absence of any commercial or financial relationships that could be construed as a potential conflict of interest.

## References

- Aa, E., Huang, W., Liu, S., Ridley, A., Zou, S., Shi, T., et al. (2018). Midlatitude plasma bubbles over China and adjacent areas during a magnetic storm on 8 September 2017. *Space Weather*. 16 (3), 321–331. doi:10.1002/2017SW001776
- Aa, E., Zou, S., Ridley, A., Zhang, S., Coster, A. J., Erickson, P. J., et al. (2019). Merging of storm time midlatitude traveling ionospheric disturbances and equatorial plasma bubbles. *Space Weather*. 17 (2), 285–298. doi:10.1029/2018SW002101
- Abdu, M. A. (2012). Equatorial spread F/plasma bubble irregularities under storm time disturbance electric fields. *J. Atmos. Sol. Terr. Phys.* 75, 44–56. doi:10.1016/j.jastp.2011.04.024
- Astafyeva, E., Zakharenkova, I., and Alken, P. (2016). Prompt penetration electric fields and the extreme topside ionospheric response to the June 22–23, 2015 geomagnetic storm as seen by the Swarm constellation. *Earth, Planet. Space* 68 (1), 152–212. doi:10.1186/s40623-016-0526-x
- Blanc, M. (1978). Midlatitude convection electric fields and their relation to ring current development. *Geophys. Res. Lett.* 5 (3), 203–206. doi:10.1029/GL005i003p00203
- Blanc, M. (1983). Magnetospheric convection effects at mid-latitudes: 3. Theoretical derivation of the disturbance convection pattern in the plasmasphere. *J. Geophys. Res. Space Phys.* 88 (A1), 235–251. doi:10.1029/JA088iA01p00235
- Blanc, M., and Richmond, A. D. (1980). The ionospheric disturbance dynamo. *J. Geophys. Res.* 85 (A4), 1669–1686. doi:10.1029/JA085iA04p01669
- Chakrabarty, D., Rout, D., Sekar, R., Narayanan, R., Reeves, G. D., Pant, T. K., et al. (2015). Three different types of electric field disturbances affecting equatorial ionosphere during a long-duration prompt penetration event. *J. Geophys. Res.* 120 (6), 4993–5008. doi:10.1002/2014JA020759
- Chakrabarty, D., Sekar, R., Sastri, J. H., and Ravindran, S. (2008). Distinctive effects of interplanetary electric field and substorm on nighttime equatorial F layer: a case study. *Geophys. Res. Lett.* 35 (19). doi:10.1029/2008GL035415
- Chandra, H., and Rastogi, R. G. (1974). Geomagnetic storm effects on ionospheric drifts and the equatorial E s, over the magnetic equator. *Indian J. Radio Space Phys.* 3 (4), 332–336. Available at: <http://nopr.niscair.res.in/handle/123456789/37843>.
- Fejer, B. G. (1991). Low latitude electrodynamic plasma drifts: a review. *J. Atmos. Terr. Phys.* 53 (8), 677–693. doi:10.1016/0021-9169(91)90121-M
- Fejer, B. G. (1997). The electrodynamics of the low-latitude ionosphere: recent results and future challenges. *J. Atmos. Sol. Terr. Phys.* 59 (13), 1465–1482. doi:10.1016/s1364-6826(96)00149-6
- Fejer, B. G. (2002). Low latitude storm time ionospheric electrodynamics. *J. Atmos. Sol. Terr. Phys.* 64 (12–14), 1401–1408. doi:10.1016/S1364-6826(02)00103-7
- Fejer, B. G. (2011). Low latitude ionospheric electrodynamics. *Space Sci. Rev.* 158 (1), 145–166. doi:10.1007/s11214-010-9690-7
- Fejer, B. G., Blanc, M., and Richmond, A. D. (2017). Post-storm middle and low-latitude ionospheric electric fields effects. *Space Sci. Rev.* 206, 407–429. doi:10.1007/s11214-016-0320-x
- Fejer, B. G., and Emmert, J. T. (2003). Low-latitude ionospheric disturbance electric field effects during the recovery phase of the 19–21 October 1998 magnetic storm. *J. Geophys. Res. Space Phys.* 108 (A12), 10190. doi:10.1029/2003JA010190
- Fejer, B. G., Farley, D. T., Balsley, B. B., and Woodman, R. F. (1976). Radar studies of anomalous velocity reversals in the equatorial ionosphere. *J. Geophys. Res.* 81 (25), 4621–4626. doi:10.1029/JA081i025p04621
- Fejer, B. G., Gonzales, C. A., Farley, D. T., Kelley, M. C., and Woodman, R. F. (1979). Equatorial electric fields during magnetically disturbed conditions 1. The effect of the interplanetary magnetic field. *J. Geophys. Res.* 84 (A10), 5797–5802. doi:10.1029/JA084iA10p05797
- Fejer, B. G., Jensen, J. W., Kikuchi, T., Abdu, M. A., and Chau, J. L. (2007). Equatorial ionospheric electric fields during the November 2004 magnetic storm. *J. Geophys. Res. Space Phys.* 112 (A10), A10304. doi:10.1029/2007JA012376
- Fejer, B. G., Jensen, J. W., and Su, S. Y. (2008). Quiet time equatorial F region vertical plasma drift model derived from ROCSAT-1 observations. *J. Geophys. Res. Space Phys.* 113 (A5), 12801. doi:10.1029/2007JA012801
- Fejer, B. G., Larsen, M. F., and Farley, D. T. (1983). Equatorial disturbance dynamo electric fields. *Geophys. Res. Lett.* 10 (7), 537–540. doi:10.1029/GL010i007p00537
- Fejer, B. G., and Navarro, L. A. (2022). First observations of equatorial ionospheric electric fields driven by storm-time rapidly recurrent magnetospheric substorms. *J. Geophys. Res. Space Phys.* 127 (12), e2022JA030940. doi:10.1029/2022ja030940
- Fejer, B. G., Navarro, L. A., Sazykin, S., Newheart, A., Milla, M., and Condor, P. (2021). Prompt penetration and substorm effects over Jicamarca during the september 2017 geomagnetic storm. *J. Geophys. Res. Space Phys.* 126 (8), 1–11. doi:10.1029/2021JA029651
- Fejer, B. G., and Scherliess, L. (1997). Empirical models of storm time equatorial zonal electric fields. *J. Geophys. Res. Space Phys.* 102 (A11), 24047–24056. doi:10.1029/97JA02164
- Fejer, B. G., Scherliess, L., and de Paula, E. R. (1999). Effects of the vertical plasma drift velocity on the generation and evolution of equatorial spread F. *J. Geophys. Res. Space Phys.* 104 (A9), 19859–19869. doi:10.1029/1999JA900271
- Fejer, B. G., Spiro, R. W., Wolf, R. A., and Foster, J. C. (1990). Latitudinal variation of perturbation electric fields during magnetically disturbed periods-1986 SUNDIAL observations and model results. *Ann. Geophys.* 8 (6), 441–454.
- Gjerloev, J. W. (2012). The SuperMAG data processing technique. *J. Geophys. Res. Space Phys.* 117 (A9), 213. doi:10.1029/2012JA017683
- Gonzales, C. A., Kelley, M. C., Behnke, R. A., Vickrey, J. F., Wand, R., and Holt, J. (1983). On the latitudinal variations of the ionospheric electric field during magnetospheric disturbances. *J. Geophys. Res. Space Phys.* 88 (A11), 9135–9144. doi:10.1029/JA088iA11p09135
- Gonzales, C. A., Kelley, M. C., Fejer, B. G., Vickrey, J. F., and Woodman, R. F. (1979). Equatorial electric fields during magnetically disturbed conditions 2. Implications of simultaneous auroral and equatorial measurements. *J. Geophys. Res. Space Phys.* 84 (A10), 5803–5812. doi:10.1029/JA084iA10p05803
- Huang, C.-S. (2012). Statistical analysis of dayside equatorial ionospheric electric fields and electrojet currents produced by magnetospheric substorms during sawtooth events. *J. Geophys. Res. Space Phys.* 117 (A2), A02316. doi:10.1029/2011JA017398
- Huang, C.-S. (2015). Storm-to-storm main phase repeatability of the local time variation of disturbed low-latitude vertical ion drifts. *Geophys. Res. Lett.* 42 (14), 5694–5701. doi:10.1002/2015GL064674
- Huang, C.-S. (2019). Long-lasting penetration electric fields during geomagnetic storms: observations and mechanisms. *J. Geophys. Res. Space Phys.* 124 (11), 9640–9664. doi:10.1029/2019JA026793
- Huang, C.-S. (2020). Systematical analyses of global ionospheric disturbance current systems caused by multiple processes: penetration electric fields, solar wind pressure impulses, magnetospheric substorms, and ULF waves. *J. Geophys. Res. Space Phys.* 125 (9), e2020JA027942. doi:10.1029/2020JA027942
- Huang, C.-S., Sazykin, S., Chau, J. L., Maruyama, N., and Kelley, M. C. (2007). Penetration electric fields: efficiency and characteristic time scale. *J. Atmos. Sol. Terr. Phys.* 69 (10–11), 1135–1146. doi:10.1016/j.jastp.2006.08.016
- Huang, C.-S., and Zhang, Y. (2021). Equatorial plasma drifts during the magnetic storm on november 7–11, 2004: identifications of the roles of penetration and disturbance dynamo electric fields with multi-instrumental measurements. *J. Geophys. Res. Space Phys.* 126 (9), e2021JA029386. doi:10.1029/2021JA029386
- Kelley, M. C. (1989). *The earth's ionosphere: electrodynamics and plasma Physics*. San Diego, Calif: Academic.
- Kelley, M. C., Fejer, B. G., and Gonzales, C. A. (1979). An explanation for anomalous equatorial ionospheric electric fields associated with a northward turning of the interplanetary magnetic field. *Geophys. Res. Lett.* 6 (4), 301–304. doi:10.1029/GL006i004p00301

## Publisher's note

All claims expressed in this article are solely those of the authors and do not necessarily represent those of their affiliated organizations, or those of the publisher, the editors and the reviewers. Any product that may be evaluated in this article, or claim that may be made by its manufacturer, is not guaranteed or endorsed by the publisher.

- Kelley, M. C., Ilma, R. R., Nicolls, M., Erickson, P., Goncharenko, L., Chau, S., et al. (2010). Spectacular low-and mid-latitude electrical fields and neutral winds during a superstorm. *J. Atmos. Sol. Terr. Phys.* 72 (4), 285–291. doi:10.1016/j.jastp.2008.12.006
- Kelley, M. C., and Retterer, J. (2008). First successful prediction of a convective equatorial ionospheric storm using solar wind parameters. *Space Weather*. 6 (8), 381. doi:10.1029/2007SW000381
- Kikuchi, T., Araki, T., Maeda, H., and Maekawa, K. (1978). Transmission of polar electric fields to the equator. *Nature* 273 (5664), 650–651. doi:10.1038/273650a0
- Kikuchi, T., Hashimoto, K. K., Kitamura, T.-I., Tachihara, H., and Fejer, B. (2003). Equatorial counter-electrojets during substorms. *J. Geophys. Res. Space Phys.* 108 (A11), 1406. doi:10.1029/2003JA009915
- Kokubun, S., and McPherron, R. L. (1981). Substorm signatures at synchronous altitude. *J. Geophys. Res. Space Phys.* 86 (A13), 11265–11277. doi:10.1029/JA086iA13p11265
- Kudeki, E., Bhattacharyya, S., and Woodman, R. F. (1999). A new approach in incoherent scatter  $F$  region  $E \times B$  drift measurements at Jicamarca. *J. Geophys. Res. Space Phys.* 104 (A12), 28145–28162. doi:10.1029/1998JA900110
- Kuyeng, K., Scipion, D., Condor, P., Manay, E., and Milla, M. (2023). “Preliminary results of new operation mode JULIA Medium Power at JRO,” in *2023 CEDAR workshop* (San Diego, CA, USA: IGP), 25–30. Available at: <http://hdl.handle.net/20.500.12816/5441> (Accessed November 30, 2023).
- Lu, G., Goncharenko, L., Nicolls, M. J., Maute, A., Coster, A., and Paxton, L. J. (2012). Ionospheric and thermospheric variations associated with prompt penetration electric fields. *J. Geophys. Res. Space Phys.* 117 (A8). doi:10.1029/2012JA017769
- Manoj, C., and Maus, S. (2012). A real-time forecast service for the ionospheric equatorial zonal electric field. *Space Weather*. 10 (9), 825. doi:10.1029/2012SW000825
- Manoj, C., Maus, S., Lühr, H., and Alken, P. (2008). Penetration characteristics of the interplanetary electric field to the daytime equatorial ionosphere. *J. Geophys. Res. Space Phys.* 113 (A12), 13381. doi:10.1029/2008JA013381
- Maruyama, N., Richmond, A. D., Fuller-Rowell, T. J., Codrescu, M. V., Sazykin, S., Toffoletto, F. R., et al. (2005). Interaction between direct penetration and disturbance dynamo electric fields in the storm-time equatorial ionosphere. *Geophys. Res. Lett.* 32 (17), L17105. doi:10.1029/2005GL023763
- Matsushita, S. (1953). Ionospheric variations associated with geomagnetic disturbances. *J. Geomagn. Geoelectr.* 5 (4), 109–135. doi:10.5636/jgg.5.109
- Matsushita, S., and Balsley, B. B. (1973). Comments on Nishida's reply. *Planet. Space Sci.* 21 (7), 1260–1262. doi:10.1016/0032-0633(73)90211-0
- Navarro, L. A., Fejer, B. G., and Scherliess, L. (2019). Equatorial disturbance dynamo vertical plasma drifts over Jicamarca: bimonthly and solar cycle dependence. *J. Geophys. Res. Space Phys.* 124 (6), 4833–4841. doi:10.1029/2019JA026729
- Newell, P. T., and Gjerloev, J. W. (2011). Evaluation of SuperMAG auroral electrojet indices as indicators of substorms and auroral power. *J. Geophys. Res. Space Phys.* 116 (A12), A12211. doi:10.1029/2011JA016779
- Newell, P. T., Sotirelis, T., Liou, K., and Rich, F. J. (2008). Pairs of solar wind-magnetosphere coupling functions: combining a merging term with a viscous term works best. *J. Geophys. Res. Space Phys.* 113 (A4), A04218. doi:10.1029/2007JA012825
- Nicolls, M. J., Kelley, M. C., Chau, J. L., Veliz, O., Anderson, D., and Anghel, A. (2007). The spectral properties of low latitude daytime electric fields inferred from magnetometer observations. *J. Atmos. Sol. Terr. Phys.* 69 (10–11), 1160–1173. doi:10.1016/j.jastp.2006.08.015
- Nishida, A. (1968). Coherence of geomagnetic DP 2 fluctuations with interplanetary magnetic variations. *J. Geophys. Res.* 73 (17), 5549–5559. doi:10.1029/JA073i017p05549
- Rastogi, R. G. (1962). The effect of geomagnetic activity on the F2 region over central Africa. *J. Geophys. Res.* 67 (4), 1367–1374. doi:10.1029/JZ067i004p01367
- Rastogi, R. G., and Patel, V. L. (1975). Effect of interplanetary magnetic field on ionosphere over the magnetic equator. *Proc. Indian Acad. Sci.* 82 (4), 121–141. doi:10.1007/BF03046722
- Rastogi, R. G., Vyas, G. D., and Chandra, H. (1978). Geomagnetic disturbance effects on equatorial spread F. *Proc. Indian Acad. Sci., A (E P Sci.)* 87, 109–113. doi:10.1007/BF03182101
- Reddy, C. A., Somayajulu, V. V., and Devasia, C. V. (1979). Global scale electrodynamic coupling of the auroral and equatorial dynamo regions. *J. Atmos. Terr. Phys.* 41 (2), 189–201. doi:10.1016/0021-9169(79)90012-6
- Riley, P. (1994). *Electrodynamics of the low latitude ionosphere*. ProQuest Dissertations and Theses Global. Houston, TX: Rice University. Available from: <https://www.proquest.com/dissertations-theses/electrodynamics-low-latitude-ionosphere/docview/304130388/se-2> (Accessed December 4, 2023).
- Sazykin, S. (2000). *Theoretical studies of penetration of magnetospheric electric fields to the ionosphere*. ProQuest Dissertations and Theses Global. Logan, UT: Utah State University. Retrieved from: <https://www.proquest.com/dissertations-theses/theoretical-studies-penetration-magnetospheric/docview/304634273/se-2> (Accessed December 4, 2023).
- Scherliess, L., and Fejer, B. G. (1997). Storm time dependence of equatorial disturbance dynamo zonal electric fields. *J. Geophys. Res. Space Phys.* 102 (A11), 24037–24046. doi:10.1029/97JA02165
- Scherliess, L., and Fejer, B. G. (1999). Radar and satellite global equatorial F region vertical drift model. *J. Geophys. Res. Space Phys.* 104 (A4), 6829–6842. doi:10.1029/1999JA900025
- Senior, C., and Blanc, M. (1987). Convection in the inner magnetosphere-Model predictions and data. *Ann. Geophys.* 5, 405–420.
- Sori, T., Shinbori, A., Otsuka, Y., Tsugawa, T., Nishioka, M., and Yoshikawa, A. (2022). Generation mechanisms of plasma density irregularity in the equatorial ionosphere during a geomagnetic storm on 21–22 December 2014. *J. Geophys. Res. Space Phys.* 127 (5), e2021JA030240. doi:10.1029/2021JA030240
- Sousasantos, J., Rodrigues, F. S., Fejer, B. G., Abdu, M. A., Massoud, A. A., and Valladares, C. E. (2023). On the role of mild substorms and enhanced hall conductivity in the plasma irregularities onset and zonal drift reversals: experimental evidence at distinct longitudes over South America. *Earth Space Sci.* 10 (11), e2023EA003071. doi:10.1029/2023EA003071
- Spiro, R. W., and Wolf, R. A. (1984). “Electrodynamics of convection in the inner magnetosphere,” in *Magnetospheric currents*. Editor T. A. Potemra, (Washington, DC: American Geophysical Union), 247–259. doi:10.1029/GM028p0247.10.1029/gm028p0247
- Spiro, R. W., Wolf, R. A., and Fejer, B. G. (1988). Penetration of high-latitude-electric-field effects to low latitudes during SUNDIAL 1984. *Ann. Geophys.* 6, 39–50.
- Tsunomura, S. (1999). Numerical analysis of global ionospheric current system including the effect of equatorial enhancement. *Ann. Geophys.* 17, 692–706. doi:10.1007/s00585-999-0692-2
- Tsunomura, S., and Araki, T. (1984). Numerical analysis of equatorial enhancement of geomagnetic sudden commencement. *Planet. Space Sci.* 32 (5), 599–604. doi:10.1016/0032-0633(84)90109-0
- Tulasi Ram, S., Yokoyama, T., Otsuka, Y., Shiokawa, K., Sripathi, S., Veenadhari, B., et al. (2016). Duskside enhancement of equatorial zonal electric field response to convection electric fields during the St. Patrick's Day storm on 17 March 2015. *J. Geophys. Res. Space Phys.* 121 (1), 538–548. doi:10.1002/2015JA021932
- Veenadhari, B., Kikuchi, T., Kumar, S., Ram, S. T., Chakrabarty, D., Ebihara, Y., et al. (2019). Signatures of substorm related overshielding electric field at equatorial latitudes under steady southward IMF Bz during main phase of magnetic storm. *Adv. Space Sci.* 64 (10), 1975–1988. doi:10.1016/j.asr.2019.04.001
- Wei, Y., Zhao, B., Guozhu, L., and Wan, W. (2015). Electric field penetration into Earth's ionosphere: a brief review for 2000–2013. *Sci. Bull.* 60 (8), 748–761. doi:10.1007/s11434-015-0749-4
- Wolf, R. A. (1970). Effects of ionospheric conductivity on convective flow of plasma in the magnetosphere. *J. Geophys. Res.* 75 (25), 4677–4698. doi:10.1029/JA075i025p04677
- Wolf, R. A., Harel, M., Spiro, R. W., Voigt, G. H., Reiff, P. H., and Chen, C. K. (1982). Computer simulation of inner magnetospheric dynamics for the magnetic storm of July 29, 1977. *J. Geophys. Res. Space Phys.* 87 (A8), 5949–5962. doi:10.1029/JA087iA08p05949
- Woodman, R. F. (1970). Vertical drift velocities and east-west electric fields at the magnetic equator. *J. Geophys. Res.* 75 (31), 6249–6259. doi:10.1029/JA075i031p06249